Pol. J. Environ. Stud. Vol. XX, No. X (XXXX), 1-18
DOI: *10.15244/pjoes/195781* ONLINE PUBLICATION DATE: 2025-02-28

Original Research

Quantitative Analysis of Drivers of Ecosystem Service Evolution

Yongzheng Wang[1, 2], Yanchun Pu[1], Haoran Yu[3]*, Xinchen Gu[4,5]**

[1]School of Architecture and Planning, Anhui Jianzhu University, Hefei, 230601, China
[2]Collaborative Innovation Center for Urbanization Construction of Anhui Province, Anhui Jianzhu University, Hefei 230601, China.
[3]School of Landscape Architecture, Nanjing Forestry University, Nanjing, 210037, China
[4]School of Civil Engineering, Tianjin University, Tianjin, 300072, China
[5]Institute of Water Resources and Hydropower Research, Beijing, 100044, China

Received: 5 August 2024
Accepted: 10 November 2024

Abstract

Intensive human activities and climate change have led to the degradation of regional ecosystem functions. Accurately assessing the dynamics of ecosystem services and their driving factors is essential for developing differentiated ecological management strategies and supporting regional sustainable development. However, understanding the responses of ESs' drivers across different spatial scales in various geographic contexts remains limited. This study focuses on the Hefei Metropolitan Area, utilizing the InVEST model to evaluate changes in four ESs: water yield, soil retention, carbon storage, and habitat quality from 2000 to 2022. The Optimal Parameter Geodetector (OPGD) model was employed to quantify the driving factors at different spatial scales. The results reveal a general decline in water yield, soil retention, and carbon storage, while habitat quality has improved. The spatial distribution of ESs exhibits a pattern of "high in the west, low in the east; high in the south, low in the north." Natural factors predominantly influence the changes in water yield and soil retention, while human activities significantly impact the spatial variation of carbon storage and habitat quality. The optimal spatial scale for detecting driving factors is 7~8 km. The findings provide a theoretical basis for optimizing ecological space in rapidly urbanizing areas.

Keywords: ecosystem services, driving factors, land use/cover change, time and space evolution, optimal parameters-based geographical detector model

Introduction

Ecosystem services (ESs) refer to the benefits provided to humans by ecosystems through their structures, functions, and operational processes [1-3]. The sustainable development of human society is inseparable from the essential support provided by ecosystems [4, 5]. In recent decades, under the

*e-mail: yuhr@njfu.edu.cn
**e-mail: gxc@tju.edu.cn

combined effects of complex climate changes and intensifying human activities, global ecosystems have been experiencing varying degrees of degradation, posing an increasing threat to human well-being [6, 7]. Therefore, to ensure the sustainable development and effective management of ESs, it is crucial to investigate the spatiotemporal characteristics of ESs and quantify the driving factors.

Since the 21st century, the study of ESs has become a focus across multiple academic disciplines. Scholars both domestically and internationally have explored ESs from different perspectives, including research on various regions, scales, and types of ESs. Their efforts have led to significant academic achievements in understanding spatiotemporal evolution patterns [8, 9], interaction relationships [10, 11], assessment techniques and methodologies [12-14], and optimization strategies [15, 16]. Assessments of ESs are primarily based on models such as emergy evaluation [17], value assessment [18], ARIES [19], SoIVES [20], and InVEST [21]. Currently, the InVEST model is most widely applied for the dynamic evaluation and spatiotemporal analysis of ESs due to its high efficiency in data processing and ease of use [22].

Common methods for identifying and quantifying the driving factors of ESs include multiple regression models [23], structural equation models [24], and the geographical detector [25]. The Geographical Detector model is widely used to examine spatial heterogeneity in geographical phenomena and analyze the interactions among driving factors, and it has been frequently employed to detect ES drivers [26, 27]. However, the traditional Geographical Detector model often relies on subjective experience to manually determine the discretization methods and the number of classifications for spatial data, which can reduce accuracy [28, 29]. In contrast, the OPGD model automatically selects the most suitable discretization method and number of classifications based on the characteristics of spatial data and combines them with specific spatial scale parameters to yield more accurate and reliable results [30, 31]. Therefore, we have chosen the OPGD model to perform the quantitative analysis of driving factors.

ESs exhibit significant spatial heterogeneity. Due to the influence of the natural geographical environment, there are considerable differences in how drivers at various spatial scales respond to ESs. Currently, the analysis of driving factors has developed into a research paradigm that uses grid scales, administrative divisions, and watersheds as basic units, combined with models for quantitative analysis [32-34]. However, further exploration of the scale effects of ES drivers is needed. Moreover, the multi-scale evaluation of these factors can help assess the appropriateness of various policies and measures for regulating ecosystems [2], providing important reference value for optimizing the precise management of ecosystems.

In 2001, the United Nations launched the Millennium Ecosystem Assessment project, which proposed a conceptual framework that clarifies the interactions between ESs and human well-being. It pointed out that ecosystems primarily provide humans with benefits through provisioning services, regulating services, supporting services, and cultural services. Based on this framework, and considering the actual development of the Hefei Metropolitan Area as well as relevant research findings [35, 36], this study selects four ESs for evaluation: water yield (WY), carbon sequestration (CS), soil retention (SR), and habitat quality (HQ). The goals of this study are: (1) to reveal the spatiotemporal heterogeneity of the four types of ESs; (2) to analyze the differences in influencing factors at different spatial scales and identify the optimal parameters; and (3) to determine the primary factors driving changes in ESs based on the optimal parameters.

Materials and Methods

Study Area

The Hefei Metropolitan Area consists of seven prefecture-level cities and one county-level city, covering a total area of 63,500 Km^2 (Fig. 1). It serves as a crucial hub for the Yangtze River Delta's expansion toward central and western China, playing an important role as a connecting link. This region has a subtropical monsoon climate with distinct seasons, and its topography is primarily composed of hills and plains. From 2000 to 2022, the GDP of the Hefei Metropolitan Area increased from 134.60 billion yuan to 2.87 trillion yuan, representing nearly 20-fold growth. During the same period, the area of developed land nearly doubled, and the population grew by 5.33 million, making it a representative case of rapid urbanization. However, as more people flock to cities, the region's ecosystem is experiencing increasing disturbances, and its high-quality development faces growing ecological risks. The functional optimization and enhancement of ESs in the metropolitan area are urgently needed.

Data Sources and Processing

All data were unified under the WGS1984-UTM-Zone-50N coordinate system with a spatial resolution of 1 km.

Selection and Treatment of Driving Factors

Changes in ESs are mainly influenced by a combination of complex factors, such as topography and geomorphology, climatic conditions, land use types, and anthropogenic activities. Referring to previous studies [40-42], and based on the data for 2020 (Table 1), we selected natural environmental factors, including elevation (X_1), slope (X_2), average annual precipitation (X_3), average annual temperature (X_4), potential evapotranspiration data (X_5), NDVI (X_6), and soil type

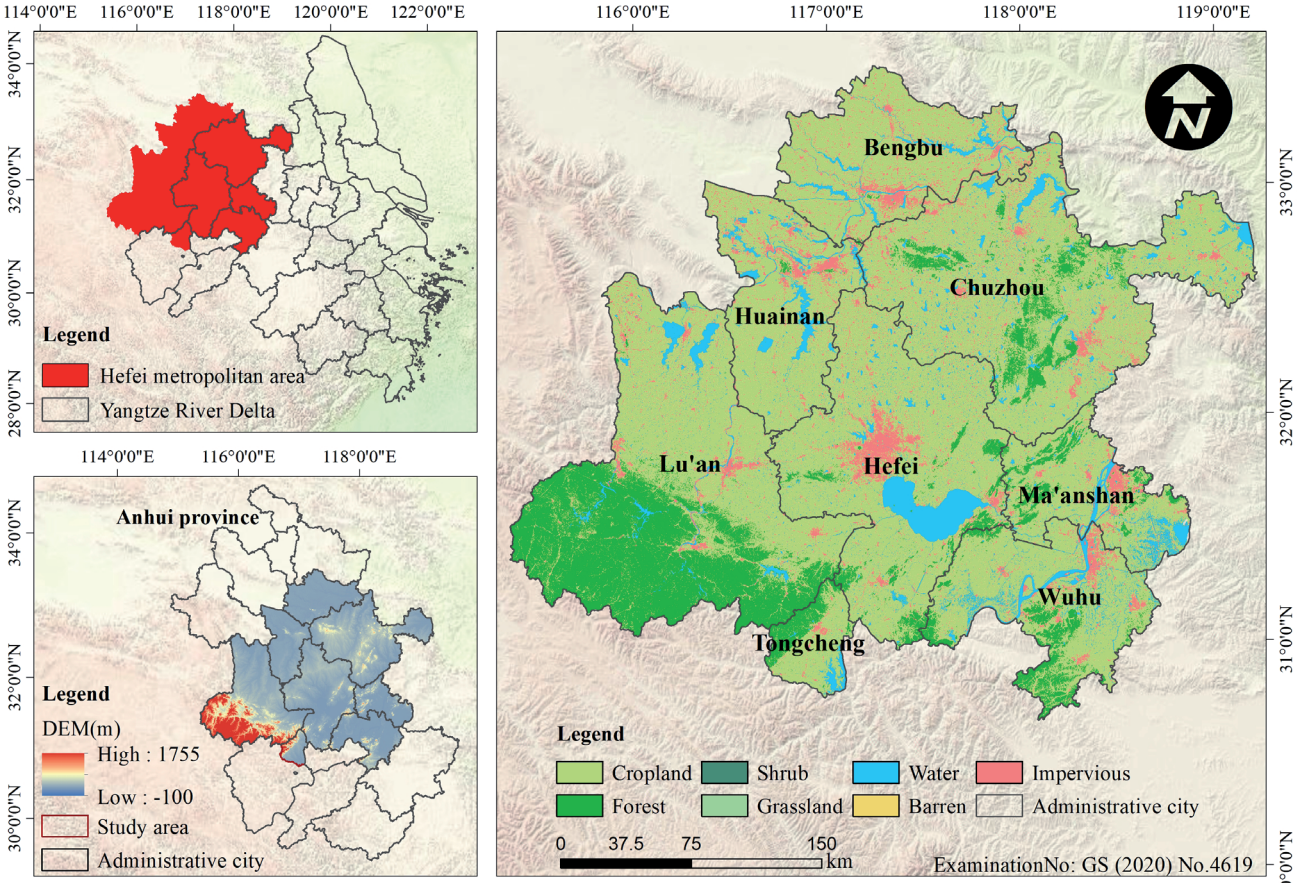

Fig. 1. Geographical location maps and land use type of the study area.

(X_7). Anthropogenic activity factors include GDP (X_8), population density (X_9), nighttime lighting data (X_{10}), land use data (X_{11}), and carbon emissions (X_{12}), totaling 12 indicators as driving factors. Then, data resolution was unified to 100×100 m, with the coordinate system set to WGS1984-UTM-Zone-50N. The water yield (WY), habitat quality (HQ), carbon sequestration (CS), and soil conservation (SR) of the 2020 Hefei Metropolitan Area were used as dependent variables for spatial differentiation driving analysis.

Research Methodology and Technical Route

Water Yield

The WY module of the InVEST model was used to assess the amount of water produced in the metropolitan area, and the equation [43] is shown below:

$$Y_{xj} = \left(1 - \frac{AET_{xj}}{P_x}\right) \times P_x \tag{1}$$

$$\frac{AET_{xj}}{P_x} = \frac{1 + W_X R_{xj}}{1 + W_X R_{xj} + \frac{1}{R_{xj}}} \tag{2}$$

$$W_X = \mathrm{z}\frac{PAWC_x}{P_x} \tag{3}$$

$$R_{xj} = \frac{K_{xj} \times ETO_x}{P_x} \tag{4}$$

where Y_{xj} is the annual WY of land use type j and raster x; AET_{xj} is the annual actual evapotranspiration of land use type j and raster x; P_x is the annual precipitation of raster x; W_x is a non physical parameter of climate-soil properties. R_x is the dryness index of land use type j and raster x, which is equal to the ratio of potential evapotranspiration and precipitation; ETO_x is the annual potential evapotranspiration of raster x; K_{xj} is the evapotranspiration coefficient of vegetation; $PAWC_x$ is the water content of plants; and z is the seasonal constant. Combined with the actual situation and concerning related studies [44], z was assigned to 6.5 (2000), 5.8 (2005), 5.3 (2010), 4.5 (2015), 5.6 (2020), and 6.3 (2022) for the water yield of each period from 2000 to 2022, respectively.

Carbon Storage

The carbon sequestration module in the InVEST model was used to quantify the carbon sequestration services in the Hefei Metropolitan Area, and the carbon

Table 1. List of data sources.

Data types	Spatial resolution	Data sources
CLCD data [32]	30 m	China's Land-Use/Cover Datasets (https://doi.org/10.5281/zenodo.8176941)
Monthly potential evapotranspiration dataset [33]	1 km	1-km monthly potential evapotranspiration dataset in China (1901-2022) (http://loess.geodata.cn)
Monthly precipitation dataset [34]	1 km	1-km monthly precipitation dataset for China (1901-2022) (http://loess.geodata.cn)
Annual average temperature [35]	k	ERA5-Land dataset (https://cds.climate.copernicus.eu)
ASTER GDEM	30 m	Geospatial data cloud (https://www.gscloud.cn/)
Normalized difference Vegetation index (NDVI) dataset [36]	1 km	MODIS/Terra Vegetation Indices Monthly L3 Global 1km SIN GridV006 (https://lpdaac.usgs.gov)
Gross domestic product (GDP) dataset [37]	1 km	(https://github.com/thestarlab/ChinaGDP)
Soil type dataset, Soil dataset [38]	1 km	Harmonized World Soil Database version 2.0 (https://www.iea.org/data-and-statistics)
Population density dataset, nighttime lighting dataset [39]	1 km	An extended time-series (2000-2023)of global NPP-VIIRS-like nighttime light data (https://dataverse.harvard.edu/)
	500 m	
CO_2 emissions dataset [40]	0.1°	EDGAR-Emissions Database for Global Atmospheric Research (https://www.iea.org/data-and-statistics)

pool data required by the model are empirical, and this study draws on the results of previous research to determine the parameters of carbon pools in different land classes [45]. The calculation formula [46] is shown below:

$$C_{tot} = C_{above} + C_{below} + C_{soil} + C_{dead} \quad (5)$$

where C_{tot} is total carbon sequestration; C_{above} is carbon sequestration by above-ground organisms; C_{below} is carbon sequestration by below-ground organisms; C_{soil} is carbon sequestration in soil; and C_{dead} is CS in dead organic matter.

Habitat Quality

The HQ Evaluation Module of the InVEST model was used to quantify HQ in the Hefei Metropolitan Area using the following formulae [47]:

$$Q_{xj} = H_j \left[1 - \left(\frac{D_{xj}^z}{D_{xj}^z + k^z}\right)\right] \quad (6)$$

where Q_{xj} is the HQ index of x raster in landscape type j; H_j represents the habitat suitability score of a landscape type, with a value range of [0,1]; k is the half-saturation constant; z is the scale constant, which was set to 0.5 in this study. Referring to related studies [48, 49], the module parameters were set and the HQ level was classified into five grades: excellent, good, moderate, poor, and worst.

Soil Retention

The rainfall erosive force R in the Hefei Metropolitan Area was calculated using the simple equation [50] for rainfall erosive force proposed by Fujian Zhou.

$$R = \sum_{i=1}^{12} (-2.6398 + 0.3046 P_i) \quad (7)$$

where P_i is the monthly rainfall, mm; R is the rainfall erosive force, (J·cm)/(m²·h).

Soil erodibility factor K was calculated using the Erosion-Productivity Impact Calculator Model (EPIC) to calculate with the following equation [51]:

Table 2. P value and C value of different land use types.

Land Use Type	Cropland	Forests	Shrub	Grassland	Water	Barren	Impervious
P	0.15	1	1	1	0	0	0
C	0.18	0.006	0.017	0.06	0	0	0.2

$$k_{EPIC} = \{0.2 + 0.3_{exp}[-0.0256m_s(1 - m_{silt}/100)]\} \times [m_{silt}/(m_c + m_{silt})]^{0.3} \times \{1 - 0.25orgC/[orgC + exp(3.72 - 2.95orgC)]\} \times \{1 - 0.7(1 - m_s/100)/\{(1 - m_s/100) + exp[-5.51 + 22.9((1 - m_s/100))]\}\} \quad (8)$$

where K_{EPIC} denotes the soil erodibility factor and m_c, m_{silt}, m_s and $orgC$ are the percentage content (%) of clay grains (<0.002 mm), chalk grains (0.002 mm to 0.05 mm), sand grains (0.05~2 mm) and organic carbon, respectively.

The sediment transport ratio module of the InVEST model was applied to calculate the soil conservation services in the Hefei Metropolitan Area. Equations [52] are given below:

$$RKLS_n = R_n \times K_n \times L_n \times S_n \quad (9)$$

$$USLE_n = R_n \times K_n \times L_n \times S_n \times C_n \times P_n \quad (10)$$

$$SK_n = RKLS_n - USLE_n \quad (11)$$

where $RKLS_n$ is the potential soil erosion (t); $USLE_n$ is the actual soil erosion (t); SK_n is the SR (t); R_n is the erosive power of rainfall; K_n is the soil erodibility; L_n is the slope length factor; S_n is the slope gradient factor; C_n is the vegetation cover and management factor; and P_n is the factor of soil and water conservation measures. C_n and P_n are assigned regarding the related studies [53-55], as shown in Table 2.

Driving Factor Analysis

Geodetector, as an analysis method used to identify the spatial differentiation of geographic features and potential influencing factors, is influenced by the discrete method of spatial data, partition effect, and spatial scale effect, all of which have an important impact on detection accuracy. Referring to the existing studies [56] and combining the scope of the study area, a spatial grid of 10 scales was constructed for detection analysis. The OPGD model was used to process the driving factors at different spatial scales. Referring to the previous study [28, 29], the classification number of the driving factors was set to be 3-7 categories, and five discrete methods, namely, the equal breaks, the natural breaks, the quantile breaks, the geometric breaks, and the standard deviation breaks, were used to detect the explanatory power q-value of each driving factor. Finally, the 90% quantile of the explanatory variables q of each driving factor at the 10 spatial scales was compared. When the quantile reached its maximum, it represented the optimal parameter combination for data discretization, and the corresponding spatial grid was identified as the optimal scale.

The effects of influencing factors on the spatial differentiation of ESs in the Hefei Metropolitan Area were analyzed using the factor detection and interaction detection of the Optimal Parameter Geodetector (OPGD) model with the following equation [57].

$$q = 1 - \frac{1}{N_\sigma^2}\sum_{i=1}^{L} N_i \sigma_i^2 \quad (12)$$

where q is the detection value of the influence of the driving factor on the spatial differentiation of ESs; q is within the [0,1] range, with larger q values indicating a stronger influence of the factors on explaining changes in ESs. N and N_i are the number of units in stratum i and the whole region, respectively. σ_i^2 and σ^2 represent the variance of the data for each level of the unit and the change in the dependent variable of all research units, respectively. L is the Y or X of the stratification.

Research Framework

The study will be implemented in three distinct phases. (1) Data preparation phase: Processing of multiple sources of data and harmonization of coordinates and data types. (2) ESs assessment stage: Based on the current situation of the Hefei Metropolitan Area, a quantitative evaluation of four types of ESs was conducted using the InVEST model. The supply capacity and spatial differentiation characteristics of various types of ESs were analyzed in terms of land-use types and administrative districts. (3) Driver factor identification stage: Initially, 12 influencing factors were selected and 10 different spatial probing scales were established. Thereafter, the Optimal Parameter Geodetector (OPGD) model was employed for single-factor detection and interactive detection with each of the four types of ESs. Then, the 90% quartiles of the 12 influencing factors were compared among the four types of ESs across the 10 types of spatial scales. In the end, the optimal parameter combinations for discretization and the optimal spatial scales for detection will be identified.

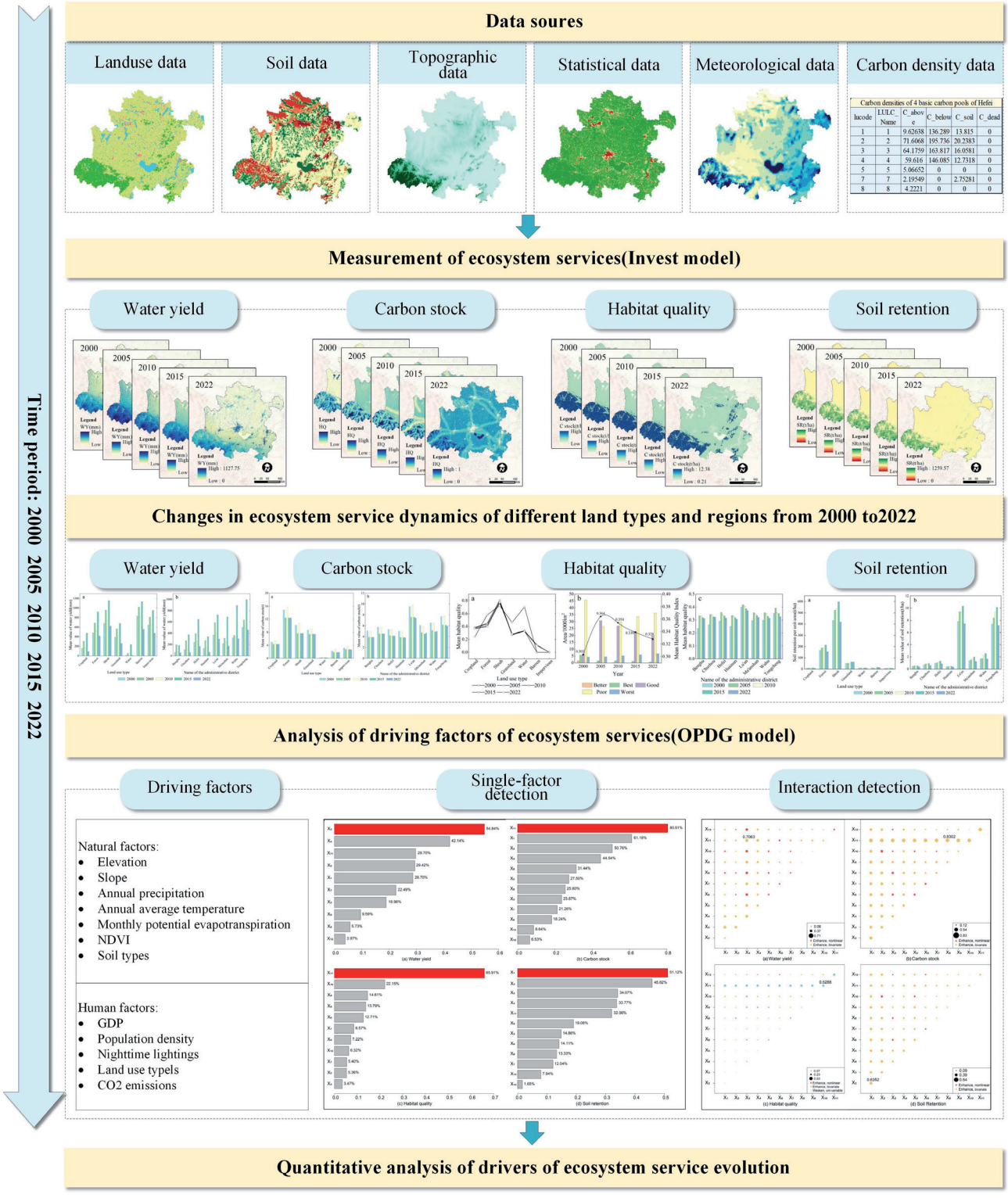

Fig. 2. Technical routes.

Results

Land Use Dynamics

Table 3 indicates that arable, forest, and building land constitute the majority of land in the Hefei metropolitan region. Between 2000 and 2022, land use changes included a significant increase in forest and building land, accompanied by declines in arable land, grassland, watersheds, bare land, and shrubland. Arable land experienced the largest area decline, 2338.92 km², while bare land saw the highest percentage decrease at 94.76%. Grassland and water bodies saw moderate declines, with shrubland experiencing the least decrease. Building land

Table 3. Land use changes in the Hefei Metropolitan Area from 2000 to 2022 (km², %).

Year	Type	Cropland	Forest	Shrub	Grassland	Water	Impervious	Barren
2000	Area	45827.48	9335.81	0.79	25.86	3988.11	4200.78	8.28
	Proportions	72.30	14.73	0.001	0.04	6.29	6.63	0.01
2005	Area	44599.86	9954.51	0.69	21.32	4330.11	4476.14	4.48
	Proportions	70.36	15.70	0.001	0.03	6.83	7.06	0.01
2010	Area	43808.14	10029.24	0.51	20.65	4394.59	5132.57	1.41
	Proportions	69.11	15.82	0.0008	0.03	6.93	8.10	0.002
2015	Area	43207.48	9861.26	0.41	16.21	4428.08	5873.15	0.53
	Proportions	68.16	15.56	0.0006	0.03	6.99	9.27	0.0008
2022	Area	43488.57	9528.72	0.35	8.16	3838.98	6587.82	0.4336
	Proportions	68.54	15.02	0.00	0.01	6.05	10.38	0.0007
2000-2005	Quantity of change	-1227.62	618.70	-0.10	-4.54	342.00	275.36	-3.80
	Rate of change	-2.68	6.63	-12.86	-17.55	8.58	6.56	-45.89
2005-2010	Quantity of change	-791.72	74.74	-0.18	-0.67	64.48	656.43	-3.07
	Rate of change	-1.78	0.75	-26.35	-3.14	1.49	14.67	-68.55
2010-2015	Quantity of change	-600.66	-167.99	-0.10	-4.44	33.49	740.58	-0.88
	Rate of change	-1.37	-1.67	-20.23	-21.49	0.76	14.43	-62.57
2015-2022	Quantity of change	281.09	-332.53	-0.05	-8.05	-589.09	714.66	-0.09
	Rate of change	0.65	-3.37	-13.03	-49.65	-13.30	12.17	-17.78
2000-2022	Quantity of change	-2338.92	192.91	-0.44	-17.70	-149.13	2387.04	-7.85
	Rate of change	-5.10	2.07	-55.47	-68.43	-3.74	56.82	-94.76

exhibited the highest growth during the study period, signaling a significant expansion in construction areas.

According to the Sankey diagram of land use transfer (Fig. S1), mutual shifts between farmland, forestland, waterways, and construction land dominate land use transfer in the Hefei metropolitan region between 2000 and 2022. Among these, the transfer of watershed and forestland diminishes over time, whereas the transfer of arable land and building land increases over time. Less than 1% of shrubs, grassland, and bare ground were converted to forestland, farmland, and construction land, respectively. Over 22 years, the Hefei metropolitan region underwent a total land-use transition encompassing 7448.91 km². Of this, 4763.21 km² of arable land transferred primarily to forestland, representing the largest change. The largest influx involved construction land, totaling 3248.57 km², a transfer ratio of 43.61%, primarily from cultivated land, forest, and water bodies. The transferred area of 864.24 km² demonstrates a notable expansion trend.

Spatiotemporal Variations in ESs

Water Yield

WY in the Hefei Metropolitan Area during the periods from 2000 to 2022 recorded at 1.61×10^{10} m³, 2.67×10^{10} m³, 1.75×10^{10} m³, 3.98×10^{10} m³, and 1.22×10^{10} m³, respectively. The long-term average was 2.25×10^{10} m³. This service demonstrated a decreasing trend, culminating in a decrease of 0.39×10^{10} m³. According to Fig. 3a) and Fig. 4, low-water yield areas, predominantly arable lands with scant precipitation and lakes, contrast with high-yield areas dominated by forested and constructed lands. The higher water yield in constructed areas primarily results from their significantly hardened subsurfaces, affecting water flow variability, including infiltration, evaporation, and surface runoff [58, 59]. Conversely, river waters exhibit lower yields mainly due to elevated evapotranspiration. The spatial distribution of water yield, as shown in Fig. 4, illustrates a gradual reduction from south to north over 2000 to 2022, with mountainous regions outperforming hills and plains. Fig. 3b) and Fig. 4 reveal that areas like Jinzhai County, Huoshan County, Shucheng County, and Tongcheng City in Lu'an, located in the southwestern Ta-pieh Mountains, where dense forests and high rainfall prevail, constitute

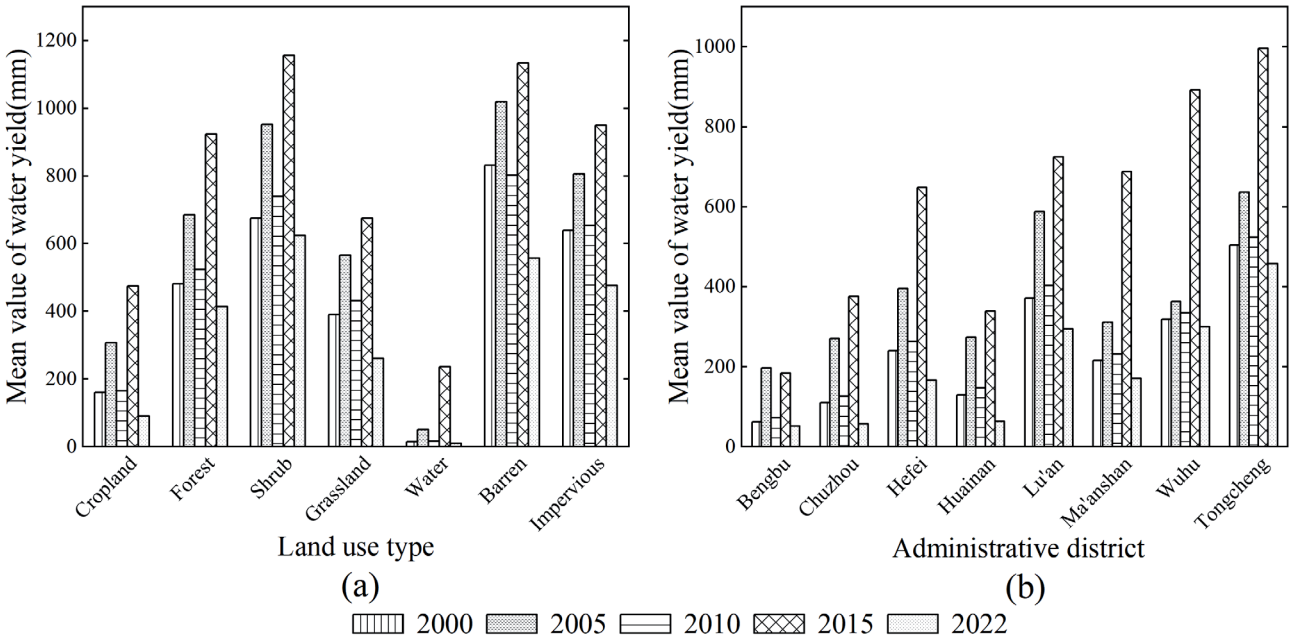

Fig. 3. Characteristics of spatial and temporal changes in WY from 2000 to 2022. a) WY for each land-use type; b) Regional differences in WY.

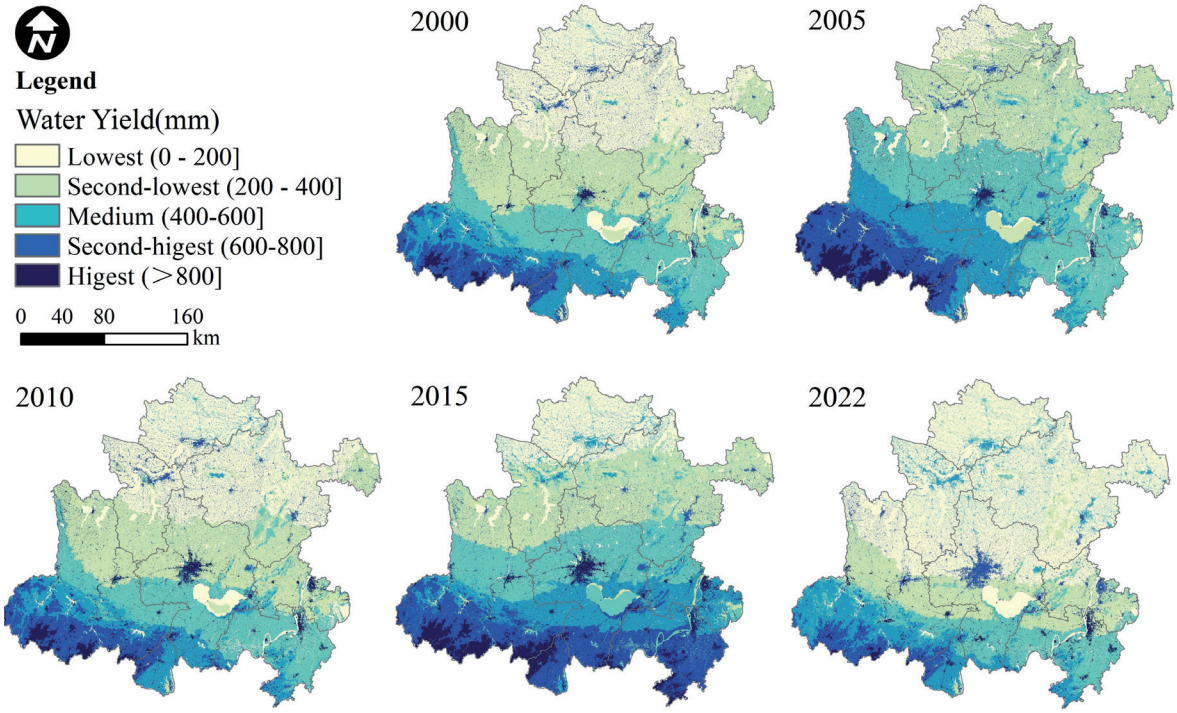

Fig. 4. Spatial pattern of WY in the Hefei Metropolitan Area from 2000 to 2022.

the highest yield zones. The Yangtze River Basin, including cities like Hefei, Wuhu, and Ma'anshan, represents the secondary high-yield zone, while the northern plains of Anhui, such as Bengbu, Huainan, and Chuzhou, are identified as low-yield areas.

Carbon Sequestration

From 2000 to 2022, the average annual CS in the Hefei metropolitan area shows a general decreasing trend, from 44.23 to 36.58. Fig. 5a) indicates that forestland holds the highest mean CS, succeeded by shrubs, grassland, cropland, and finally water, which records the lowest values. Significant variations in the

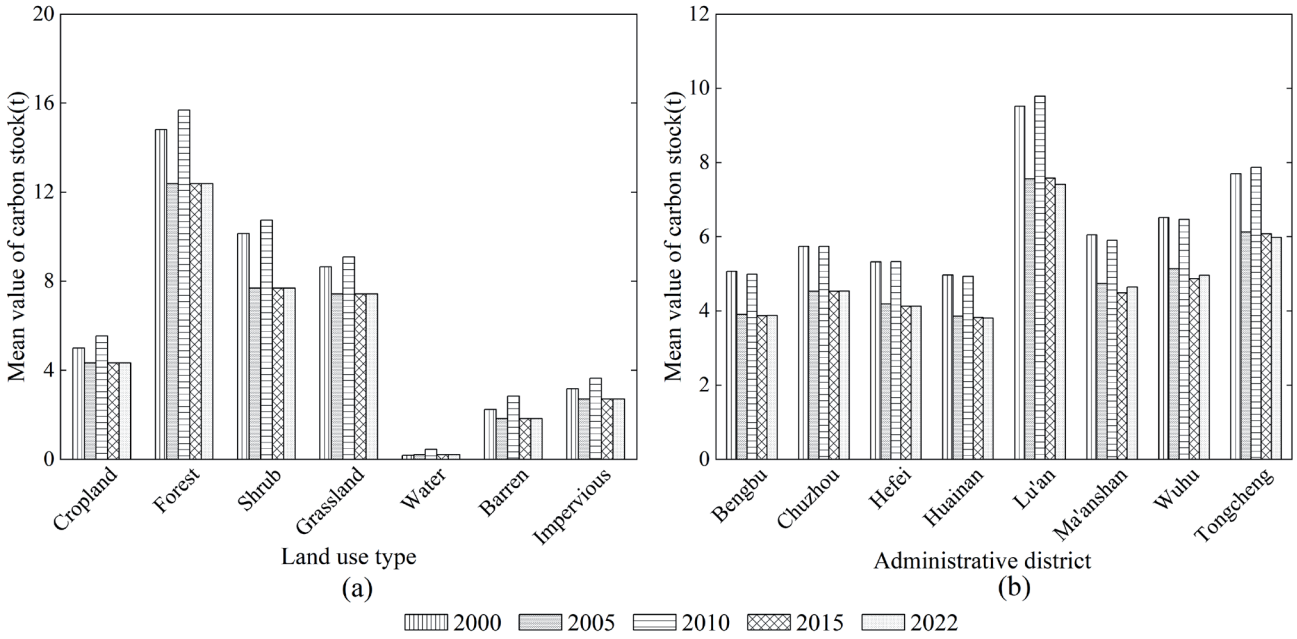

Fig. 5. Characteristics of spatial and temporal changes of CS, 2000-2022. a) CS per unit area for each land-use type; b) Regional differences in CS.

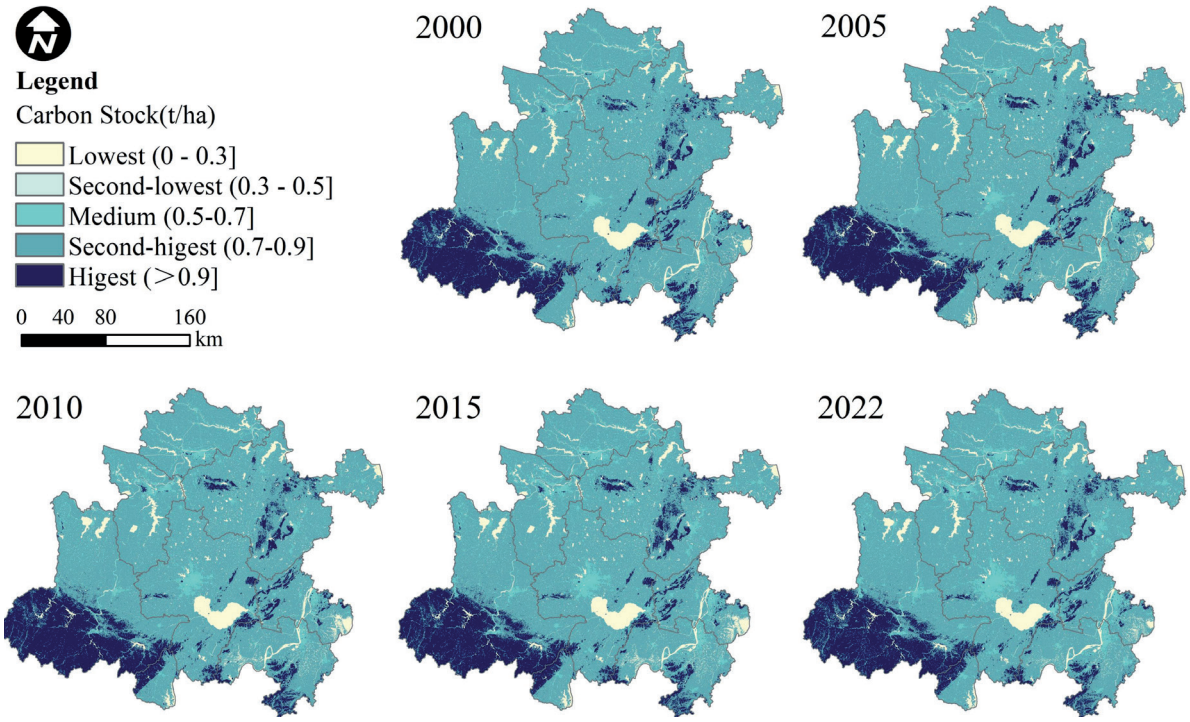

Fig. 6. Spatial pattern of CS in the Hefei Metropolitan Area from 2000 to 2022.

total annual CS across different categories were noted, with construction land showing the largest increase from 1.16×10^7 t in 2000 to 1.99×10^7 t in 2022, an increase of 71.72%. Conversely, bare land experienced the most substantial reduction, decreasing by 94.51%. Spatially, CS in the Hefei Metropolitan Area is higher in the south than in the north, and mountainous areas surpass the plains. Fig. 5b) and Fig. 6 reveal that high values of CS predominantly occur in the central region of Chuzhou City, the southern areas of Lu'an City, the northwestern segments of Tongcheng City, and the southern reaches of Wuhu City, areas characterized by dense forest cover. Low-value areas mainly lie in the plains, where arable land, water bodies, and construction sites are prevalent.

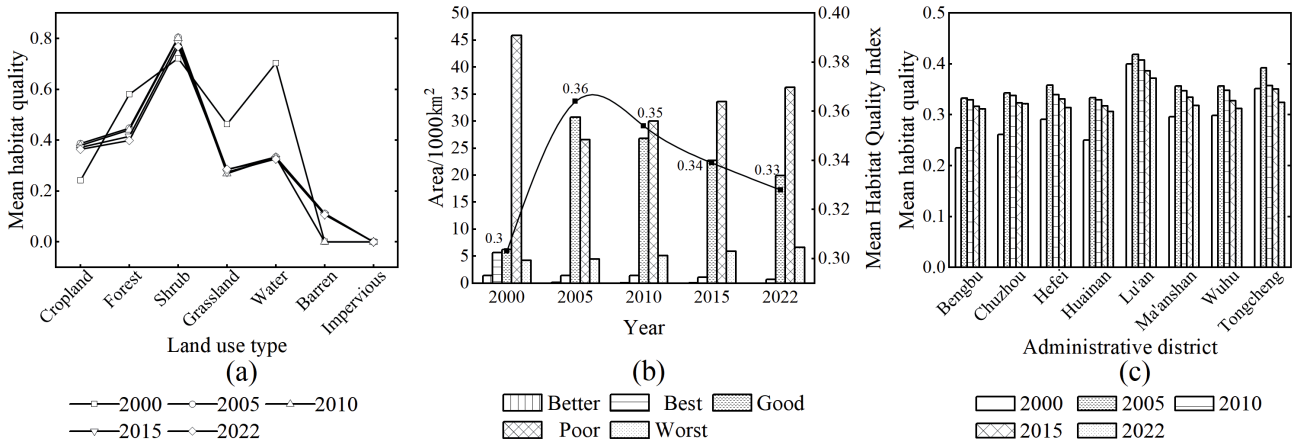

Fig. 7. Characteristics of spatial and temporal changes of HQ from 2000 to 2022. a) Mean value of HQ for each land-use type; b) Area of each class of HQ and the HQI; c) Regional differences in HQ.

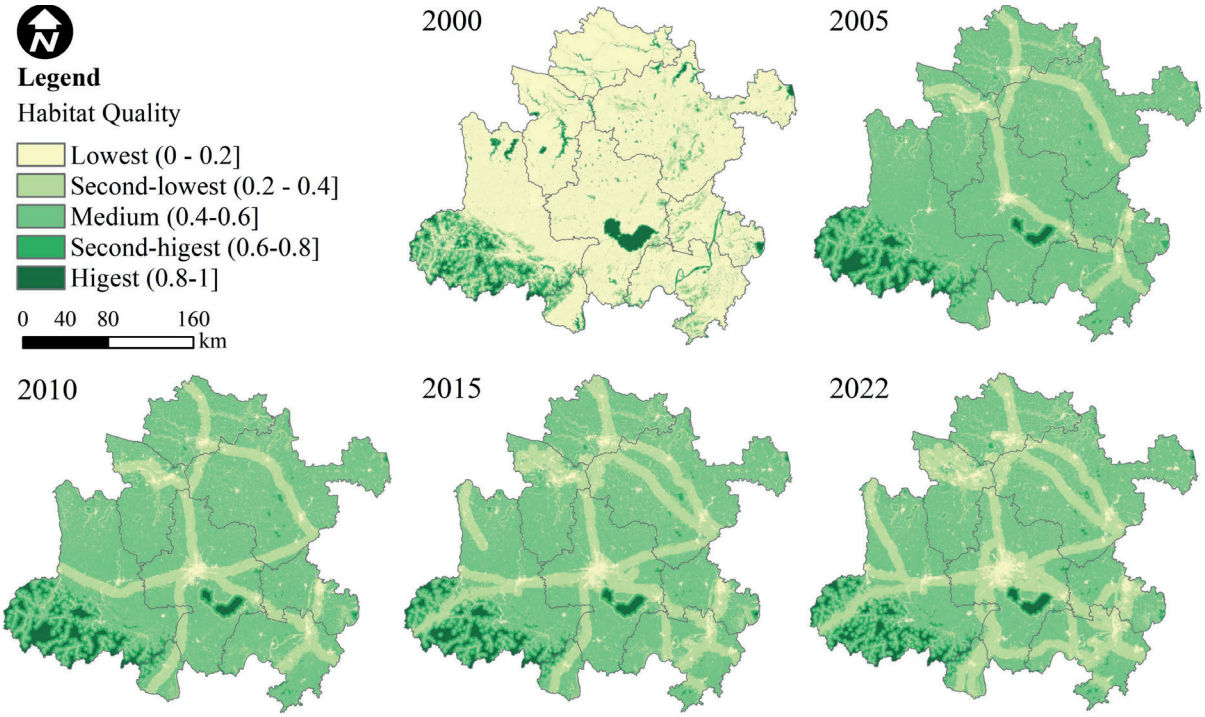

Fig. 8. Spatial pattern of HQ in the Hefei Metropolitan Area from 2000 to 2022.

Habitat Quality

The HQ of the Hefei Metropolitan Area is classified into five grades: excellent (0.8–1), good (0.6–0.8), moderate (0.4–0.6), poor (0.2–0.4), and worst (0–0.2). From 2000 to 2022, the average indices of habitat quality (HQI) in the Hefei metropolitan area were 0.303, 0.364, 0.354, 0.334, and 0.328, respectively, showing a general upward trend. According to Fig. 7b), the areas with excellent and good HQ decreased over time, while moderate quality areas initially increased and then decreased; poor quality areas decreased and then increased, and worst quality areas consistently increased. Between 2000 and 2022, the most substantial changes in HQ percentages occurred in the moderate and poor classes, whereas the excellent, good, and worst classes saw less fluctuation. Spatially, as depicted in Fig. 7, excellent and good habitat qualities are predominantly situated in the Ta-pieh Mountains, the hilly regions of Chuzhou City, and riverside areas. Conversely, poor-quality habitats are primarily located in urban and transportation corridor proximities. Fig. 7a) and Fig. 8 suggest that habitats in woodland and water-rich areas generally exhibit higher quality indices, often exceeding 0.6, with some areas achieving values as high as 0.9.

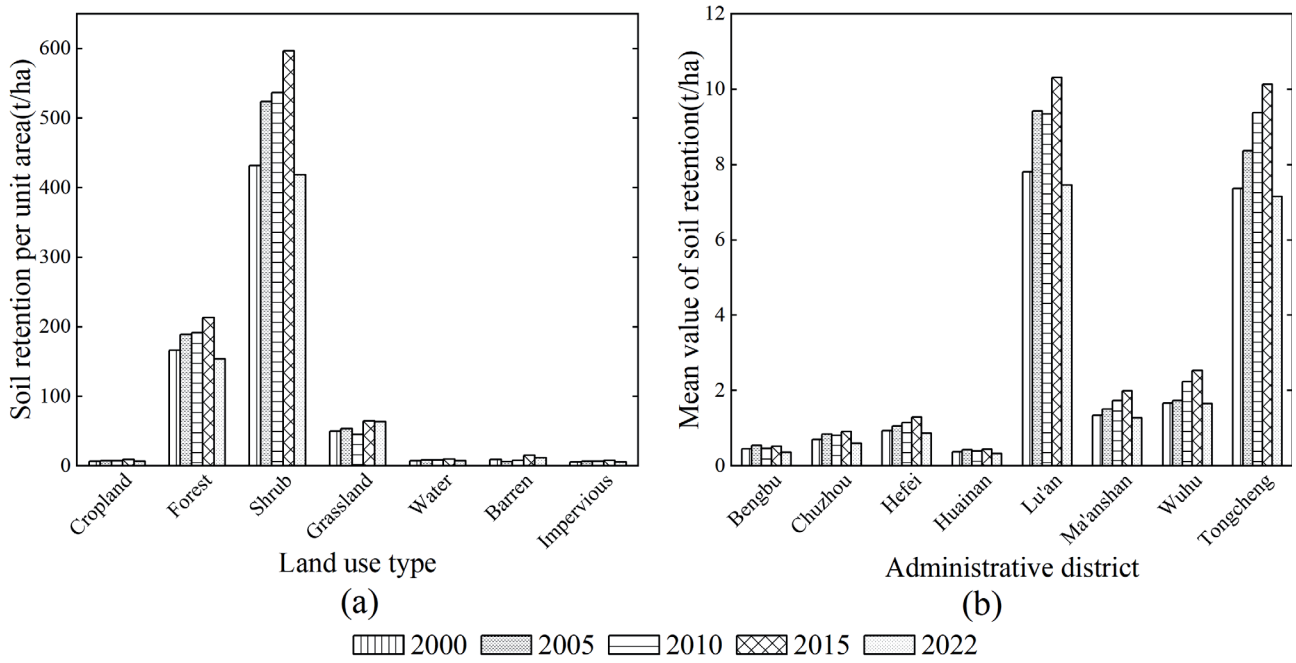

Fig. 9. Characteristics of spatial and temporal changes of SR from 2000 to 2022. a) SR per unit area for each land-use type; b) Regional differences in SR.

Soil Retention

From 2000 to 2022, SR in the Hefei Metropolitan Area recorded values of 1.92×10^8 t, 2.27×10^8 t, 2.31×10^8 t, 2.57×10^8 t and 1.81×10^8 t, respectively. The multi-year average was 2.18×10^8t, displaying an initial increase followed by a decrease. According to Fig. 9a), shrublands and woodlands exhibit high SR capacities, surpassing those of grasslands, while croplands and built-up areas show lower capacities. Over the 2000–2022 period, the soil conservation capacity per unit area of forest land decreased by 12.69 t/hm², experiencing the most substantial reduction at 36.50%, with bare land following, and minimal changes observed in other land types. Fig. 10 illustrates that high soil conservation areas are predominantly located in the hilly and mountainous western regions, characterized by dense forest cover and steep terrain gradients, where soil conservation services are more effective. Integrating data from Fig. 9b), it is apparent that Lu'an City and Tongcheng City feature the highest soil conservation rates, followed by Hefei, Ma'anshan, and Wuhu City, while Bengbu, Chuzhou, and Huainan display comparatively lower rates. This pattern indicates that increased land use intensity in the plains correlates with reduced ecosystem service provision.

Analysis of Drivers of Ecosystem Service Changes

Optimal Parameter Identification

The same driving factors exhibit varied effects on the four types of ESs across different spatial regions. The analysis indicated that each of the 12 factors influenced the spatial dynamics of the ESs to varying degrees (Fig. S2). As the spatial grid cells used for detection increased in size, the q-values of most driving factors generally rose and then stabilized. An analysis of ten sets of grid cells, designed for factor detection, showed that the 90% quantile of the explanatory variable q-values for WY, CS, HQ, and SR reached their maximum at grid sizes of 8 km, 7 km, 8 km, and 7 km, respectively. Consequently, these grid sizes are identified as the optimal spatial resolutions for assessing the drivers of spatial differentiation in these ESs.

The explanatory power, as measured by q-values, varies significantly across different combinations of discretization methods and the number of driver breakpoints (Fig. S3 and Fig. S4). According to Fig. S3a) and Fig. S4a), slope and GDP displayed the highest q-values when the data was divided into 7 intervals using geometric breaks. Similarly, potential evapotranspiration and soil type were segmented into 7 intervals with natural breaks, while precipitation and nighttime light used equal breaks. Elevation, NDVI, and carbon emissions were categorized into 6 intervals using geometric, equal, and quantile breaks, respectively. The optimal parameters for population density and land use type combined geometric breaks with 5 intervals, and the air temperature was discretized into 5 intervals using natural breaks. The driver discretization of CS, HQ, and SR followed the same approach as WY.

Drivers Analysis

Single-factor detection shows that both natural conditions and anthropogenic activities influence the spatial heterogeneity of the four ESs to varying

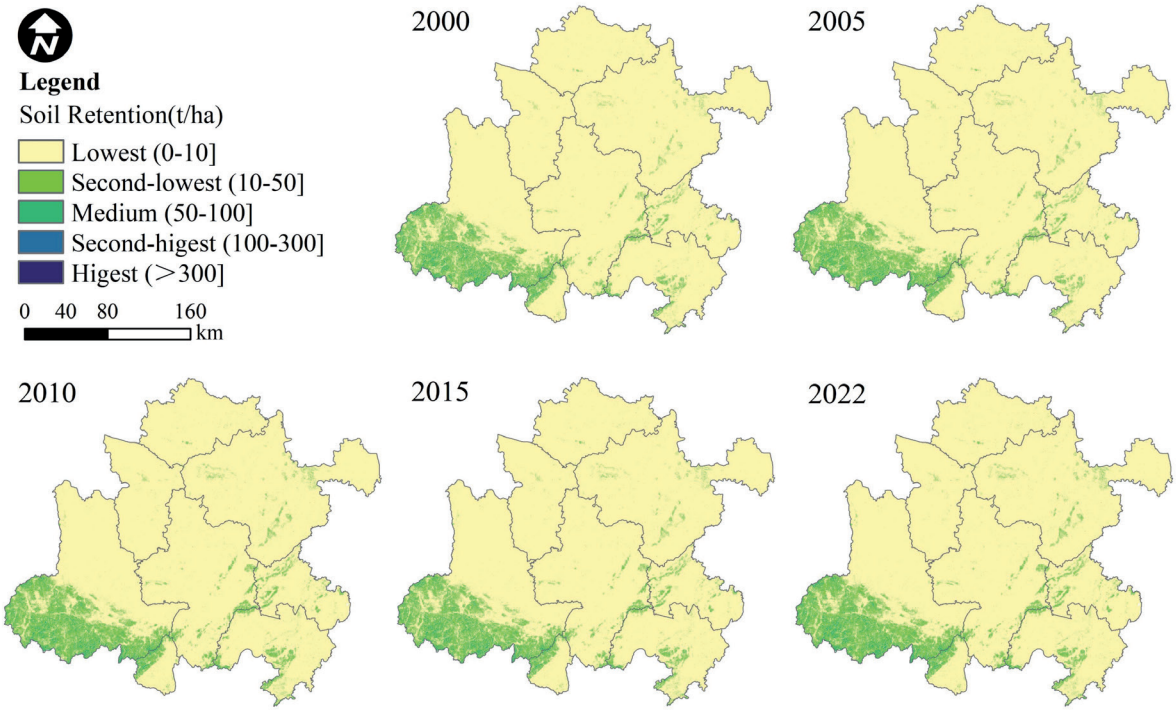

Fig. 10. Spatial pattern of SR in the Hefei Metropolitan Area from 2000 to 2022.

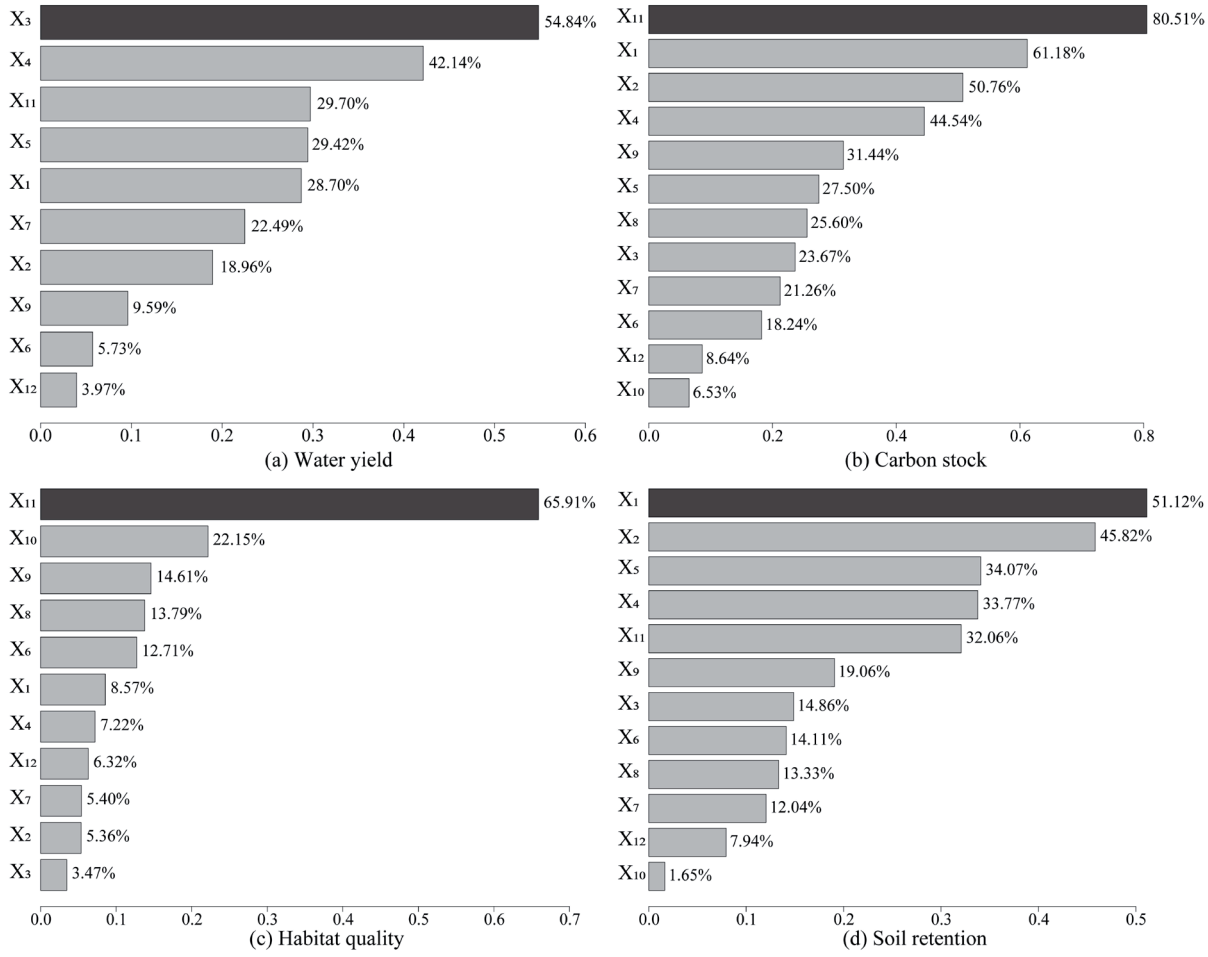

Fig. 11. Detecting the impact of a single factor on ESs change using the OPGD model.

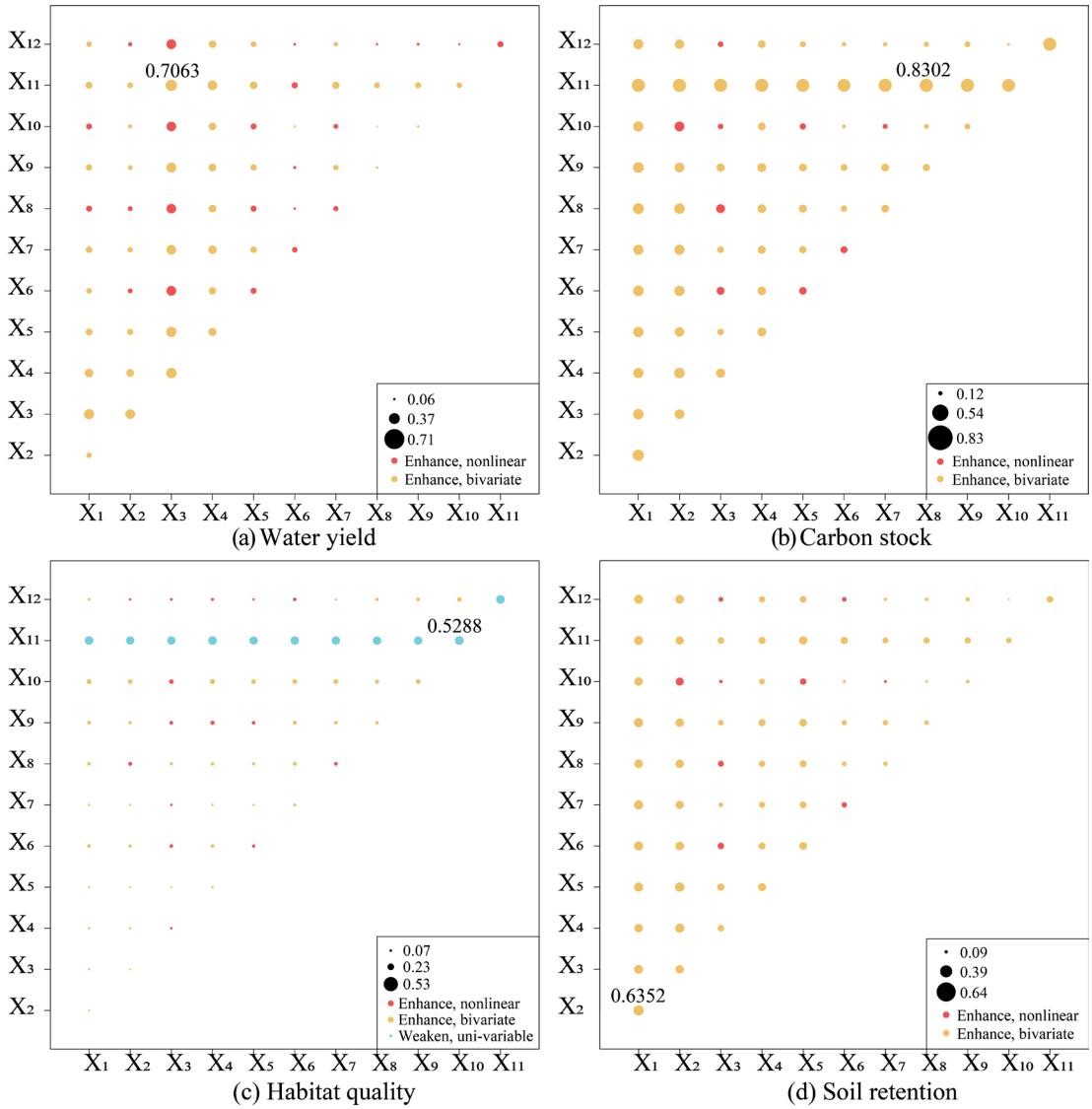

Fig. 12. Detecting the impact of drivers on ecosystem service change using OPGD model interactions.

extents. Fig. 11a) reveals that annual precipitation (X_3), temperature (X_4), land use type (X_{11}), potential evapotranspiration (X_5), and elevation (X_1) are the predominant factors affecting the spatial variability in water yield, with explanatory powers of 54.84%, 42.14%, 29.70%, 29.42%, and 28.70%, respectively. In contrast, GDP (X_8) and nighttime lighting (X_{10}) show no significant correlation. Fig. 11b) demonstrates that all twelve factors impact the spatial differentiation of carbon stocks differently. Land use type (X_{11}), elevation (X_1), slope (X_2), temperature (X_4), and population density (X_9) are significant, with q-values of explanatory power above 30%, and land use type alone contributes up to 80.51%, indicating a dominant influence. Fig. 11c) highlights that nighttime lighting (X_{10}) and land use type (X_{11}) are critical in influencing the spatial heterogeneity of HQ, with explanatory powers of 65.91% and 22.15%, respectively, significantly impacted by human activities. Fig. 11d) details how the spatial distribution of SR is primarily determined by elevation (X_1), slope (X_2), potential evapotranspiration (X_5), air temperature (X_4), and land use type (X_{11}), with respective explanatory powers of 51.12%, 45.82%, 34.07%, 33.77%, and 32.06%. This pattern indicates a strong correlation between SR and topographic relief, climatic conditions, and land use type. Collectively, land use patterns, topography, and meteorological factors are the principal drivers of spatial heterogeneity in ESs in the Hefei Metropolitan Area.

Interaction detection results reveal that pairwise interactions among factors significantly influenced the spatial differentiation of ESs in the Hefei Metropolitan Area, more so than individual factors alone. These interactions also varied considerably in their contributions to the explanatory power of different types of ESs. Fig. 12a) indicates that interactions included 23 pairs of nonlinear enhancements and 43 pairs of two-factor enhancements in water yield. Rainfall (X_3) and temperature (X_4) demonstrated the strongest interactions with other factors, achieving explanatory power q-values above 40%. Notably, interactions involving land use type

(X_{11}) and rainfall (X_3) surpassed 60% strength, with the combination of land use type and rainfall reaching the highest at 70.63%. This pattern suggests that rainfall, potential evapotranspiration, air temperature, and land use type are pivotal in driving the spatial variability of water yield. Fig. 12b) reveals that interactions in carbon stock primarily involved two-factor enhancements, with 9 pairs showing nonlinear enhancement and 57 pairs showing two-factor enhancement. Land use type exhibited the most substantial interactions, with q-values above 80%, where land use type (X_{11}) combined with GDP (X_8) yielded an explanatory power of 83.02%. This indicates that anthropogenic activities significantly affect the spatial distribution of carbon stocks, with notable interactions also involving elevation, slope, and meteorological factors. Fig 12c) demonstrates that HQ interaction results included 40 pairs of two-factor enhancements, 15 pairs of nonlinear enhancements, and 11 pairs of one-factor nonlinear attenuation. The interaction involving land use type (X_{11}) and nighttime lighting (X_{10}) emerged as the most influential, with a q-value of 52.88%, indicating a substantial anthropogenic impact on HQ. Fig. 12d) depicts that SR interactions featured 9 pairs of nonlinear enhancements and 57 pairs of two-factor enhancements. The interactions between elevation (X_1) and slope (X_2) were particularly potent, contributing significantly to SR's spatial heterogeneity with a q-value of 63.52%. This suggests that topographic factors predominantly influence SR, alongside notable contributions from land use type, temperature, and potential evapotranspiration.

Discussion

Characterizing the Spatial and Temporal Evolution of ESs

Over the past 20 years, the spatial distribution of similar types of ESs has exhibited a high degree of consistency, generally displaying the pattern of "higher in the west and south, lower in the east and north, with mountainous areas higher than hills and plains", which is closely related to changes in land use structure. Changes in WY, CS, and SR show significant differences, while HQ has changed the least (Fig. S5). Overall, WY, SR, and CS have declined, while HQ has increased [60]. In terms of the spatial distribution of ES, there are clear differences at both the administrative district scale and land use type level. At the administrative district level, Lu'an City, Tongcheng City, Ma'anshan City, and Wuhu City are high-value areas for ES. Among these, SR exhibits the most significant differences between city and county levels, while HQ shows the least variation. This is mainly because SR's spatial distribution is primarily controlled by topographic relief [61], whereas HQ is more strongly related to the land use pattern [36]. Land use changes are mainly reflected in the conversion of farmland to construction land around urban areas, and the changes are not significant at the city and county level. The differences in ES across land use types are mainly reflected in the stronger ES supply capacity of forests, shrubs, and grasslands compared to other land types, with areas where these land types are concentrated naturally becoming high-value areas for ES [21]. Therefore, in the process of regional development and construction, the focus should be on highly intensive, efficient, and high-quality land use functions, promoting the formation of a land use model that integrates production, living, and ecological functions in a complementary and synergistic manner, while avoiding the disorderly expansion of urban construction space.

Influencing Factors of ESs

The study selected both natural environmental factors and socio-economic factors for the quantitative analysis of ESs' drivers. Overall, changes in WY and SR were primarily driven by the natural geographic environment, while the spatial distribution of CS and HQ was more significantly influenced by human activities, particularly the constraints imposed by land use types on their spatial patterns, consistent with the findings of Wang's study [36]. Among these, CS and SR were more sensitive to variations in terrain and slope [62], while climatic factors such as rainfall, temperature, and evapotranspiration contributed to the spatial heterogeneity of WY [63]. HQ, on the other hand, followed socio-economic changes, as the expansion of construction land driven by socio-economic development altered regional ecosystems' climate conditions, vegetation cover, species distribution, and biodiversity, resulting in HQ degradation [34]. This suggests that, in addition to climate conditions and the natural environment, land use patterns, production and living practices, and policy measures closely tied to human activities also play a crucial role in the spatiotemporal evolution of ESs. Therefore, accurately quantifying the factors influencing regional ESs and understanding how ecosystems respond to human activities, as well as the feedback mechanisms involved, can better promote high-quality regional development [64, 65].

The response of ESs' influencing factors to spatial scale exhibits significant variability. As the detection scale changes, the intensity of influencing factors on ESs also shifts. Across 10 different spatial grid settings, as the grid scale increases, the spatial aggregation of influencing factors grows, and the spatial distribution of ESs becomes more closely related to the influencing factors, making their driving effects more pronounced. When the grid scale reaches a certain threshold, the influence of the factors peaks, but beyond this critical point, the effect weakens. This indicates that there is an optimal spatial scale parameter for the impact of influencing factors. Our study, using the OPGD model, confirmed that the drivers of ESs exhibit a significant

scale effect across different spatial scales. A more refined scale helps accurately identify differences in the spatial distribution of various ESs, allowing for more precise management of ESs, and ultimately achieving refined control of land use patterns [31, 32]. Therefore, the fine-scale protection and management of regional ecosystems should take into account the spatial scale effects of various influencing factors, with particular attention to the optimal scale of factor impact. At the same time, the interaction of multiple influencing factors across different spatial scales must also be considered. By fully utilizing the intensity of drivers at different spatial scales to regulate the supply capacity of ESs, it is possible to maximize the ecological service benefits in different regions.

Limitations and Future Research

The study employed the Optimal Parameter Geoprobe (OPGD) model to analyze the drivers of spatial differentiation in ESs and to explore the partitioning and scale effects of spatial data. Compared to the traditional Geodetector model, the OPGD model enhances the discretization methods, results, and the number of partitions in the spatial data, which leads to more reliable detection outcomes and more accurately reflects the role of the driving factors in the spatial heterogeneity of ESs. Ecosystems, however, are complex and vast, influenced by interlinked social, economic, and natural factors. The complexity of their interactions presents a significant scientific challenge in dissecting and quantifying the influence of multiple factors. The study's reliance on relevant literature for data calculations impacts the accuracy of the results. Furthermore, the analysis of driving factors is limited to the interactions between paired factors, failing to address the influence of multiple factors on the dependent variable, nor does it consider whether the effect of the influencing factors is positive or negative. Future research should employ a variety of methods to examine the mechanisms and relationships among influencing factors.

Conclusions

This study conducted a quantitative analysis of ESs in the Hefei Metropolitan Area with the InVEST model, and further explored the dominant drivers affecting their spatial heterogeneity through the OPGD model. The findings are as follows:

(1) From 2000 to 2022, WY, SR, and CS declined overall, while HQ increased. The spatial distribution showed a consistent pattern: higher in the south and west, lower in the north and east, with mountainous areas having greater values than plains and hills.

(2) The results of the OPGD model indicate that a grid scale of 7~8 km is the optimal spatial scale for exploring the driving factors of ESs in the Hefei Metropolitan Area.

(3) Single-factor detection highlighted that land use patterns, topography, and meteorological factors are the primary influencers of spatial differentiation among the ESs. Interactive detection revealed that natural factors primarily drove changes in WY and SR, while human activities more significantly affected CS and HQ.

Acknowledgments

Research and demonstration of key technologies for the construction of park cities in the megacity Shanghai (grant number: 23DZ1204400).

Conflict of Interest

The authors declare no conflict of interest.

References

1. BISHOP J., BRINK P.T., GUNDIMEDA H., KUMAR P., NESSHÖVER C., SCHRÖTER-SCHLAACK C., SIMMONS B., SUKHDEV P., WITTMER H. The economics of ecosystems and biodiversity: mainstreaming the economics of nature: a synthesis of the approach, conclusions and recommendations of TEEB. Publisher UNEP. **2010**.
2. CARPENTER S.R., DEFRIES R., DIETZ T., MOONEY H.A., POLASKY S., REID W.V., SCHOLES R.J. Millennium ecosystem assessment: research needs. American Association for the Advancement of Science. **2006**.
3. COSTANZA R., D'ARGE R., DE GROOT R., FARBER S., GRASSO M., HANNON B., LIMBURG K., NAEEM S., O'NEILL R., PARUELO J. The value of the world's ecosystem services and natural capital. Nature. **387** (6630), 253, **1997**.
4. ZHANG X.F., HAN R.Q., YANG S.J., YANG Y., TANG X.T., QU W.J. Identification of bundles and driving factors of ecosystem services at multiple scales in the eastern China region. Ecological Indicators. **158**, 14, **2024**.
5. HERNÁNDEZ-BLANCO M., COSTANZA R., CHEN H.J., DEGROOT D., JARVIS D., KUBISZEWSKI I., MONTOYA J., SANGHA K., STOECKL N., TURNER K., VAN'T HOFF V. Ecosystem health, ecosystem services, and the well-being of humans and the rest of nature. Global Change Biology. **28** (17), 5027, **2022**.
6. FAROOQI T.J.A., IRFAN M., PORTELA R., ZHOU X., SHULIN P., ALI A. Global progress in climate change and biodiversity conservation research. Global Ecology and Conservation. **38**, 15, **2022**.
7. MORENO-MATEOS D., ALBERDI A., MORRIËN E., VAN DER PUTTEN W.H., RODRíGUEZ-UñA A., MONTOYA D. The long-term restoration of ecosystem complexity. Nature Ecology & Evolution. **4** (5), 676, **2020**.
8. LIU W., ZHAN J.Y., ZHAO F., WANG C., ZHANG F., TENG Y.M., CHU X., KUMI M.A. Spatio-temporal variations of ecosystem services and their drivers in the Pearl River Delta, China. Journal of Cleaner Production. **337**, 11, **2022**.
9. JIN Z., XIONG C., LUAN Q., WANG F. Dynamic

Evolutionary Analysis of Land Use/Cover and Ecosystem Service Values on Hainan Island. International Journal of Environmental Research and Public Health. **20** (1), 18, **2023**.
10. LI G.Y., JIANG C.H., GAO Y., DU J. Natural driving mechanism and trade-off and synergy analysis of the spatiotemporal dynamics of multiple typical ecosystem services in Northeast Qinghai-Tibet Plateau. Journal of Cleaner Production. **374**, 14, **2022**.
11. ALEMU I.J.B., RICHARDS D.R., GAW L.Y.F., MASOUDI M., NATHAN Y., FRIESS D.A. Identifying spatial patterns and interactions among multiple ecosystem services in an urban mangrove landscape. Ecological Indicators. **121**, 14, **2021**.
12. CORDIER M., AGÚNDEZ J.A.P., HECQ W., HAMAIDE B.A guiding framework for ecosystem services monetization in ecological-economic modeling. Ecosystem Services. **8**, 86, **2014**.
13. WU N.D., YANG Y., LIU D.X. Relevant practices for evaluating the value of overseas water ecosystem services. Water Resources Development Research. **23** (12), 14, **2023**.
14. GAO J.R., WANG K.P., XIE M.K., ZHAO Y.C., WANG X.Y., LIU C.H., ZHANG Y.L. Exploring Natural–Social Impacts on the Complex Interactions of Ecosystem Services in Ecosystem Service Bundles. Ecosystem Health and Sustainability. **10**, 0236, **2024**.
15. FU Y.J., SHI X.Y., HE J., YUAN Y., QU L.L. Identification and optimization strategy of county ecological security pattern: A case study in the Loess Plateau, China. Ecological Indicators. **112**, 10, **2020**.
16. SUN X., YANG P., TAO Y., BIAN H. Improving ecosystem services supply provides insights for sustainable landscape planning: A case study in Beijing, China. Science of the Total Environment. **802**, 13, **2022**.
17. ZHAN J.Y., ZHANG F., CHU X., LIU W., ZHANG Y. Ecosystem services assessment based on emergy accounting in Chongming Island, Eastern China. Ecological Indicators. **105**, 464, **2019**.
18. AROWOLO A., DENG X., OLATUNJI O., OBAYELU A. Assessing changes in the value of ecosystem services in response to land-use/land-cover dynamics in Nigeria. Science of the Total Environment. **636**, 597, **2018**.
19. BAGSTAD K.J., VILLA F., JOHNSON G.W., VOIGT B. ARIES–Artificial Intelligence for Ecosystem Services: A guide to models and data, version 1.0. ARIES report series. **1**, **2011**.
20. VAN RIPER C.J., KYLE G.T., SUTTON S.G., BARNES M., SHERROUSE B.C. Mapping outdoor recreationists' perceived social values for ecosystem services at Hinchinbrook Island National Park, Australia. Applied Geography. **35** (1-2), 164, **2012**.
21. YANG Q.Q., ZHANG P., QIU X.C., XU G.L., CHI J.Y. Spatial-temporal variations and trade-offs of ecosystem services in Anhui Province, China. International Journal of Environmental Research and Public Health. **20** (1), 855, **2023**.
22. NDONG G., VILLERD J., COUSIN I., THEROND O. Using a multivariate regression tree to analyze trade-offs between ecosystem services: Application to the main cropping area in France. Science of the Total Environment. **764**, 12, **2021**.
23. LI W., WANG L., YANG X., LIANG T., ZHANG Q., LIAO X., WHITE J., RINKLEBE J. Interactive influences of meteorological and socioeconomic factors on ecosystem service values in a river basin with different geomorphic features. Science of the Total Environment. **829**, 9, **2022**.
24. DUOLAITI X., KASIMU A., REHEMAN R., AIZIZI Y., WEI B.H. Assessment of water yield and water purification services in the arid zone of northwest China: The case of the Ebinur Lake Basin, Land. **12** (3), 533, **2023**.
25. CHENG C., LIU Y.L., LIU Y.F., YANG R.F., HONG Y.S., LU Y.C., PAN J.W., CHEN Y.Y. Cropland use sustainability in Cheng–Yu Urban Agglomeration, China: Evaluation framework, driving factors and development paths. Journal of Cleaner Production. **256**, 120692, **2020**.
26. WANG J.F., XU C.D. Geodetector: Principle and prospective. Acta Geographica Sinica. **72** (1), 19, **2017**.
27. YANG D., LIU W., TANG L.Y., CHEN L., LI X.Z., XU X.L. Estimation of water provision service for monsoon catchments of South China: Applicability of the InVEST model. Landscape and Urban Planning. **182**, 133, **2019**.
28. ZHAO X.Y., TAN S.C., LI Y.P., WU H., WU R.J. Quantitative analysis of fractional vegetation cover in southern Sichuan urban agglomeration using optimal parameter geographic detector model, China. Ecological Indicators. **158**, 15, **2024**.
29. SONG Y.Z., WANG J.F., GE Y., XU C.D. An optimal parameters-based geographical detector model enhances geographic characteristics of explanatory variables for spatial heterogeneity analysis: cases with different types of spatial data. GIScience & Remote Sensing. **57**, (5), 593, **2020**.
30. ZHANG R., CHEN Y., ZHANG X.F., FANG X., MA Q., REN L. Spatial-temporal Pattern and Driving Factors of Flash Flood Disasters in Jiangxi Province Analyzed by Optimal Parameters-Based Geographical Detector. Geographical Geo-Information. **37**, 72, **2021**.
31. LI C., QIAO W.F., GAO B.P., CHEN Y. Unveiling spatial heterogeneity of ecosystem services and their drivers in varied landform types: Insights from the Sichuan-Yunnan ecological barrier area. Journal of Cleaner Production. **442**, 14, **2024**.
32. XIA H., YUAN S.F., PRISHCHEPOV A.V. Spatial-temporal heterogeneity of ecosystem service interactions and their social-ecological drivers: Implications for spatial planning and management. Resources, Conservation and Recycling. **189**, 106767, **2023**.
33. WANG X.Z., WU J.Z., LIU Y.L., HAI X.Y., SHANGUAN Z.P., DENG L. Driving factors of ecosystem services and their spatiotemporal change assessment based on land use types in the Loess Plateau. Journal of environmental management. **311**, 114835, **2022**.
34. FANG L.L., WANG L.C., CHEN W.X., SUN, J., CAO Q., WANG S.Q., WANG L.Z. Identifying the impacts of natural and human factors on ecosystem service in the Yangtze and Yellow River Basins. Journal of Cleaner Production. **314**, 127995, **2021**.
35. PENG J., TIAN L., LIU Y.X., ZHAO M.Y., HU Y.N., WU J.S. Ecosystem services response to urbanization in metropolitan areas: Thresholds identification. Science of the Total Environment. **607**, 706, **2017**.
36. WANG Y.Z., GU X.C., YU H.R. Spatiotemporal variation in the Yangtze River Delta Urban agglomeration from 1980 to 2020 and future trends in ecosystem services. Land. **12** (4), 929, **2023**.
37. ZHAO N.Z., LIU Y., CAO G.F., SAMSON E.L., ZHANG J.Q. Forecasting China's GDP at the pixel level using nighttime lights time series and population images. GIScience & Remote Sensing. **54**, (3), 407, **2017**.
38. International Institute for Applied Systems Analysis. Harmonized World Soils Database version 2.0. Available

online: https://pure.iiasa.ac.at/id/eprint/17595/ (accessed on 25 December **2023**).
39. IEA-International Energy Agency. Available online: https://www.iea.org/data-and-statistics (accessed on 15 February **2024**).
40. SCHIRPKE U., TASSER E., BORSKY S., BRAUN M., EITZINGER J., GAUBE V., GETZNER M., GLATZEL S., GSCHWANTNER T., KIRCHNER M. Past and future impacts of land-use changes on ecosystem services in Austria. Journal of Environmental Management. **345**, 118728, **2023**.
41. KANKAM S., OSMAN A., INKOOM J.N., FÜRST C. Implications of spatio-temporal land use/cover changes for ecosystem services supply in the coastal landscapes of Southwestern Ghana, West Africa. Land. **11** (9), 1408, **2022**.
42. ZHANG W. Discussion on urban water ecological management model in Anhui Province. Water Resources Development Research. **228** (6), 32, **2020**.
43. ZHANG H.J., PANG Q., HUA Y.W., LI X.X., LIU K. Linking ecological red lines and public perceptions of ecosystem services to manage the ecological environment: A case study in the Fenghe River watershed of Xi'an. Ecological Indicators. **113**, 14, **2020**.
44. LI Y.Y., MA X.S., QI G.H., WU Y.L. Studies on water retention function of Anhui Province based on InVEST model of parameter localization. Resour. Environ. Yangtze Basin. **31** (2), 313, **2022**.
45. WU N., CHEN N., CHENG P., SONG T. Evaluation of carbon storage on terrestrial ecosystem responses to land cover change under five future scenarios in Anhui Province. Resources and Enoironmental in the Yangtze Basin. **32** (2), 415, **2023**.
46. YUE S.J., JI G.X., CHEN W.Q., HUANG J.C., GUO Y.L., CHENG M.Y. Spatial and Temporal Variability Characteristics of Future Carbon Stocks in Anhui Province under Different SSP Scenarios Based on PLUS and InVEST Models. Land. **12** (9), 1668, **2023**.
47. CAO Y., WANG C., SU Y., DUAN H., WU X., LU R., SU Q., WU Y., CHU Z. Study on Spatiotemporal Evolution and Driving Forces of Habitat Quality in the Basin along the Yangtze River in Anhui Province Based on InVEST Model. Land. **12** (5), 1092, **2023**.
48. SHARP R., CHAPLIN-KRAMER R., WOOD S., GUERRY A., DOUGLASS J. InVEST User's Guide. **2018**.
49. ARMOSKAITE A., AIGARS J., ANDERSONE I., HANSEN H.S., SCHRODER L., STRAKE S. Assessing change in habitat composition, ecosystem functioning and service supply in Latvian protected stony reefs. Journal of Environmental Management. **298**, 12, **2021**.
50. YU F., CHENG X.F, ZHAO M.S. Evaluation of soil erosion sensitivity in Anhui Province. Yangtze River. **40** (9), 32, **2009**.
51. WANG B., ZHENG F., GUAN Y. Improved USLE-K factor prediction: A case study on water erosion areas in China. International Soil and Water Conservation Research. **4** (3), 168, **2016**.
52. BENAVIDEZ R., JACKSON B., MAXWELL D., NORTON K. A review of the (Revised) Universal Soil Loss Equation ((R) USLE): With a view to increasing its global applicability and improving soil loss estimates. Hydrology and Earth System Sciences. **22** (11), 6059, **2018**.
53. XU S.J., DENG L., ZHAO M.S., CHEN X., SHIQI Q. Spatial-temporal characteristics of soil erosion in Anhui Province from 1980 to 2020. Science Technology and Engineering. **23** (1), 109, **2023**.
54. WANG W.Z., JIAO J.Y. Quantitative evaluation on factors influencing soil erosion in China. BULLETIN OF SOIL AND WATER CONSERVATION. **1996**.
55. ZHAO M.S., LI D.C., ZHANG G.L. Dynamic Evolution and Prediction of Soil Erosion in Anhui Province from 1980 to 2010. Soils. **48**, 588, **2016**.
56. VIDAL-ABARCA GUTIÉRREZ M.R., NICOLÁS-RUIZ N., SÁNCHEZ-MONTOYA M.D.M., SUÁREZ ALONSO M.L. Ecosystem services provided by dry river socio-ecological systems and their drivers of change. Hydrobiologia. **850** (12), 2585, **2023**.
57. XIA H., YUAN S., PRISHCHEPOV A.V. Spatial-temporal heterogeneity of ecosystem service interactions and their social-ecological drivers: Implications for spatial planning and management. Resources, Conservation and Recycling. **189**, 106767, **2023**.
58. QIAO Y.J., ZHANG H., HAN X.Y., LIU Q.B., LIU K., HU MT., PEI W.M. Exploring drivers of water conservation function variation in Heilongjiang Province from a geospatial perspective. Acta Ecologica Sinica. **43**, 2711, **2023**.
59. YAN X.Y., HUANG M.Y., TANG Y.R., GUO Q., WU X., ZHANG G.Z. Study on the Dynamic Change of Land Use in Megacities and Its Impact on Ecosystem Services and Modeling Prediction. Sustainability. **16** (13), 5364, **2024**.
60. LI N., SUN P.L., ZHANG J.Y., MO J.X., WANG K. Spatiotemporal evolution and driving factors of ecosystem services' transformation in the Yellow River basin, China. Environmental Monitoring and Assessment. **196** (3), 252, **2024**.
61. LIU Q., QIAO J.J., LI M.J., HUANG M.J. Spatiotemporal heterogeneity of ecosystem service interactions and their drivers at different spatial scales in the Yellow River Basin. Science of the Total Environment. **908**, 168486, **2024**.
62. ANSLEY R.J., RIVERA-MOMROY V.H., GRIFFIS-KYLE K., HOAGLAND B., EMERT A., FAGIN T., LOSS S.R., MCCARTHY R.H., SMITH N.G. WARING E.F. Assessing impacts of climate change on selected foundation species and ecosystem services in the South-Central USA. Ecosphere. **14** (2), e4412, **2023**.
63. YU H.R., XIAO H.W., GU X.C. Integrating species distribution and piecewise linear regression model to identify functional connectivity thresholds to delimit urban ecological corridors. Computers, Environment and Urban Systems. **113**, 102177, **2024**.
64. WANG Y.Z., JI Y.W., YU H.R., LAI X.Y. Measuring the Relationship between Physical Geographic Features and the Constraints on Ecosystem Services from Urbanization Development. Sustainability. **14** (13), 8149, **2022**.
65. SUN Y.H., HAO Z.Y., YANG Y., YE D.D., LIU J.H., LIU B.Y. Research on Beijing's water planning system based on the national space planning system. Water Resources Development Research. **2024**.

Supplementary Material

https://www.pjoes.com/SuppFile/195781/1/